Liquid-glass transition in monoatomic vanadium: A first-principles study

Pier Luigi Silvestrelli and Alberto Ambrosetti
Dipartimento di Fisica e Astronomia "G. Galilei", Università di Padova, via Marzolo 8, I-35131 Padova, Italy, and CNR-IOM Democritos, via Bonomea 265, I-34136 Trieste, Italy

(Received 28 December 2018; published 6 March 2019)

Monoatomic metallic glasses, successfully obtained in recent experiments, represent ideal systems to investigate the local atomic structures in glasses and glass-forming processes. By *ab initio* molecular dynamics we simulate the formation of a metal glass of vanadium and compute different structural, energetic, and electronic properties, including the electrical and thermal conductivities, which are compared to those of vanadium in the standard, solid-state, bcc crystal phase (obtained by adopting a slower quenching rate) and in the liquid phase too. As found for other monoatomic metallic glasses, we show that the fundamental structural process of V glass formation is represented by the tendency of V atoms to form icosahedral structures. This conclusion, together with the analysis of the electronic-charge distribution and the estimate of the electrical conductivity, suggests that the glass state of vanadium can be interpreted as a "frozen" (inherent) liquid configuration.

DOI: 10.1103/PhysRevB.99.094201

I. INTRODUCTION

Metallic glasses represent both interesting systems for fundamental theoretical investigation and very promising materials for practical applications because of their attractive mechanical properties: for instance, they are among the strongest engineering materials known (typically stronger than steel), are exceptionally elastic, and can be shaped and molded like plastics ("thermoplastic forming") [1]. In a *glassy* (or amorphous) state, in general a system has properties similar to those of a solid, but it is characterized by a disordered, liquidlike structure. When a liquid metal is cooled below its melting temperature, the resulting supercooled liquid tends to crystallize easily and quickly, so that it is generally assumed that it is impossible to cool metals into a glassy state, with the exception of certain metallic alloys which exhibit a significantly lower propensity to crystallize than pure metals [1]; in fact the glass-forming ability of a metal glass (MG) increases with the number of components, particularly if they contain elements with large atomic-size ratios. Actually, so far several complex alloys have been reported to form bulk metallic glasses; however, their multicomponent character greatly complicates the study of local atomic structures and understanding the detailed glass-forming mechanism [1].

Remarkably, the recent introduction of a general ultrarapid heating and cooling method made the vitrification of liquids of pure, monoatomic metals possible [1,2] by inducing unprecedentedly high liquid-quenching rates of the order of 10^{14} K/s (100 K/ps), thus confirming the long-standing conjecture that any metallic liquid can be vitrified into a glassy state provided that the cooling rate is sufficiently high [3,4]. The formation condition and the thermal stability of obtained monoatomic MGs were investigated by combining *in situ* transmission electron microscopy observation and simulations based on atoms-to-continuum modeling [2]. In particular, metallic glasses have been formed by considering liquid Ta, V, W, and Mo, which are refractory, early-transition, bcc metals with high melting points and excellent thermal conductivities; however, the same experimental approach failed to produce any MG from fcc metals, which are characterized by a faster crystal-growth rate [2]. Interestingly, the successful formation of MGs implies that the cooling process occurs at timescales short enough to be comparable with those typical in atomistic molecular dynamics simulations since these techniques (particularly the first-principles approaches) still have well-known restrictions in terms of sample size and timescale due to limitations in computing power. Normally, experimental samples are quenched at rates much slower than one can simulate, so that the longest realizable molecular dynamics (MD) simulations are still many orders of magnitude too short to simulate glass formation or crystallization at typical, realistic cooling rates [1].

Therefore, in view of these new experimental advances, a direct comparison between simulations and experiments is nowadays possible: in fact, MD simulations of cooling processes, which were assumed to be absolutely unrealistic to describe real phenomena, now become very useful tools to study local atomic structure in glasses and to explore the competition between glass formation and crystallization processes in pure monoatomic metals, which, in principle, represent the simplest glass formers since they are devoid of the severe complications due to the thermal effects in multicomponent MGs.

Atomic-level structures in liquid and monoatomic MG tantalum were recently investigated by Zhang *et al.* [5] using *ab initio* MD simulations, showing that the fundamental characteristic of a Ta MG is the formation of *icosahedral*-type clusters, including distorted and full icosahedrons. The structural evolution of copper during rapid quenching was also studied using *ab initio* MD simulations by Fang *et al.* [6], although, to our knowledge, the formation of a MG from Cu (which is characterized by a fcc-favored crystal structure) has not yet been experimentally realized. Both these papers were focused on the study of structural properties.

Here we investigate, using *ab initio* MD simulations, both *structural* and *electronic* properties of monoatomic vanadium in its liquid, glass, and crystalline phase. V is a *transition* metal with properties dominated by the presence of *d* electrons. Clearly, the advantage of adopting the (computationally expensive) *ab initio* approach is that atomic forces are computed from first principles, without the need for any experimental data or empirical potentials commonly used in classical MD simulation; moreover, a detailed characterization of electronic properties is possible, including an estimate of electrical and thermal conductivities. In a previous *ab initio* study [7] the conventional crystallization process of liquid V, undergoing a first-order phase transition from liquid to solid state, was simulated over a temperature range from 3000 down to 1500 K by focusing on the short-range order evolution during solidification, investigated using various structural analysis methods.

The outline of this paper is as follows. In Sec. II the adopted method is presented, and computational details are provided. In Sec. III the results of the simulations are reported and discussed. Finally, some conclusions are drawn in Sec. IV.

II. METHOD

Ab initio MD simulations were performed, within the density functional theory (DFT) framework, with the QUANTUM ESPRESSO *ab initio* package [8], by adopting a periodically repeated simple cubic box containing $N = 128$ V atoms. In order to make relatively long MD simulations possible, the sampling of the Brillouin zone (BZ) was limited to the Γ point ($k = 0$); this choice is in line with that of previous *ab initio* investigations of tantalum [5], copper [6], and V [7] and is justified by the disordered character of the studied systems (the properties of the ordered crystal phase are known and are here recomputed just for the sake of comparison). However, for a selected set of atomic configurations, a more thorough k-point sampling (with eight k points) of the BZ was adopted, according to the prescription of Monkhorst and Pack [9]. In fact, previous studies [10,11] on liquid metals such as sodium and aluminum showed that, while the Γ-point-only sampling of the BZ is generally adequate to reproduce structural properties, it can be much less accurate for the electronic ones, particularly the electrical conductivity. Electron-ion interactions were described using ultrasoft pseudopotentials with 13 (8 core + 5 valence) electrons explicitly considered. The wave functions were expanded in a plane-wave basis set with an energy cutoff of 25 Ry, and the Perdew-Burke-Ernzerhof generalized gradient approximation DFT functional [12] was adopted since it typically offers a good compromise between computational efficiency and accuracy. We have verified that the chosen energy cutoff was appropriate: for instance, the predicted equilibrium lattice constant for the bcc V crystal (using a two-atom cubic supercell with $16 \times 16 \times 16$ k-point sampling of the BZ) was 3.00 Å, in good agreement with the reference experimental value of 3.02 Å. For the calculation of the electrical conductivity, besides the eight-k-point sampling of the BZ, a higher energy cutoff of 75 Ry was also adopted for better accuracy.

In the starting configuration 128 V atoms were arranged on a crystal bcc structure, with a lattice constant of 12.08 Å, corresponding to the experimental equilibrium density of solid V. A liquid phase configuration was then obtained by equilibrating the structure for 5 ps by performing an initial simulation in which the temperature was set to 4000 K by simple velocity rescaling; this temperature was chosen to be much higher than the experimental melting temperature (2183 K) of V in order to allow the atoms to diffuse and lose memory of the initial configuration. Newton's equations were integrated using Verlet's algorithm with a MD time step of 200 a.u. (= 4.84 fs). We have verified that, at the end of such a preliminary simulation, the translational order parameter was vanishing, thus indicating complete loss of crystalline order. Subsequently, starting from the final, liquid-structure configuration, different simulations were performed by cooling the system to room temperature or below, at different quenching rates, in the range from 0.8×10^{14} to 3.1×10^{14} K/s (namely, from 78 to 313 K/ps). Final structural results were obtained by averaging over the last 600 configurations of each simulation to get a reliable statistical sample. Production simulations were performed at constant volume; however, in the final configurations, the supercell volume was relaxed in such a way to minimize the energy of the system. In principle, during the simulations, one could adjust the supercell volume to make the external pressure of the inherent structures be equal to zero, as done in Ref. [6]; however, we have verified by extensive testing that this more complex procedure is much less efficient and, in any case, does not lead to appreciable qualitative changes in the calculated properties.

In principle, partially filled d bands can give rise to striking magnetic effects [13]. However, our tests showed that this was not the case for the properties and the processes investigated in the present study [14]; spin polarization effects were found to be unimportant, so that most of the production simulations were performed using an unpolarized approach.

As in previous studies [6,7], the fundamental structures characterizing the different phases of V have been analyzed in terms of basic structural units derived from bond-pair analysis, as detailed below. Clearly, for a metallic system one of the most interesting properties is also represented by its electrical conductivity, which is here computed using the Kubo-Greenwood [15] formula and the KGEC program [16]. In this approach the electrical conductivity σ can be obtained by extrapolating to zero frequency the optical conductivity:

$$\sigma = \sigma(0) = \lim_{\omega \to 0} \sigma(\omega), \tag{1}$$

with $\sigma(\omega)$ computed as a configurational average of

$$\sigma(\omega, R_I) = \frac{2\pi e^2}{3m^2\omega} \frac{1}{V_b} \sum_{i,j} (f_i - f_j) |\langle \psi_i | \hat{p} | \psi_j \rangle|^2 \times \delta(E_j - E_i - \hbar\omega), \tag{2}$$

where e and m are the electronic charge and mass, $\hat{p}$ is the momentum operator, and ψ_i and E_i, are the electronic DFT eigenstates and eigenvalues, calculated for the ionic configuration $\{R_I\}$, at a single k point (for instance, the Γ point) of the BZ. The generalization of Eq. (2) to more than one k-vector sampling is straightforward:

$$\sigma(\omega, R_I) = \sum_{\mathbf{k}} \sigma(\omega, R_I, \mathbf{k}) \cdot W(\mathbf{k}), \tag{3}$$

where $\sigma(\omega, R_I, \mathbf{k})$ is defined by Eq. (2), with the eigenstates and the eigenvalues computed at $\mathbf{k}$, and $W(\mathbf{k})$ is the weight of point $\mathbf{k}$. Of course, the use of the single-particle DFT states and eigenvalues, instead of the true many-body eigenfunctions and eigenvalues, introduces an approximation in the calculation of σ. Due to the finite-size discretization of the eigenvalue spectrum, in practical applications $\sigma(\omega, R_I)$ is computed for a finite set of frequencies $(\omega_1, \omega_2, \ldots, \omega_l, \ldots)$ by averaging over a small frequency range $\Delta\omega$:

$$\sigma(\omega_l, R_I) \approx \frac{1}{\Delta\omega} \int_{\omega_l - \Delta\omega/2}^{\omega_l + \Delta\omega/2} \sigma(\omega, R_I) d\omega. \tag{4}$$

The value of $\Delta\omega$ must be carefully chosen. In fact it has to be large enough to ensure that a sufficient number of electronic levels contribute and, at the same time, small enough to allow good resolution. A value of $\Delta\omega = 0.15$ eV was found to be adequate for V. Since a limited number of excited states have been included in the calculation, $\sigma(\omega)$ falls off artificially fast for large values of ω; however, this does not represent a serious problem for the determination of the dc electrical conductivity $\sigma(\omega = 0)$, which is evaluated as the vanishing ω limit of $\sigma(\omega)$. While, in principle, the electrical conductivity should be computed by adopting a finite-temperature, self-consistent electronic-structure calculation [17], as in Refs. [10,11], we here adopt a more standard approach in which thermal effects on the electrons are simply included by introducing a smearing Gaussian function (appropriate to a selected temperature) and fractionally occupied electronic states [16]. This procedure is justified by the fact that we are mainly interested in systems at room temperature or below.

III. RESULTS AND DISCUSSION

Several MD simulations, characterized by different quenching rates, were performed. We report detailed results relative to two of them, as representative of a *liquid-crystal* transition (Q1) and a *liquid-glass* transition (Q2). In Q1 the quenching rate was 136 K/ps, corresponding to imposing a cooling rate of 2 K per MD time step, while in Q2 the quenching rate was 260 K/ps, corresponding to a cooling rate of 3 K per MD time step.

Figures 1 and 2 report the time evolution of the ionic temperature and the temperature dependence of the system total energy relative to the Q1 and Q2 quenching processes. For the Q1 case one can observe an evident jump in both the temperature-time and energy-temperature curves at a temperature around 2200 K, which compares favorably with the experimental melting temperature (2183 K) of V. These abrupt jumps are compatible with the first-order character of the liquid-crystal phase transition [18]. The same process was investigated by Debela *et al.* [7], who performed an *ab initio* simulation over a temperature range from 3000 down to 1500 K (using a cooling rate of 33.3 K/ps) and found that crystallization occurs at 1600 K in supercooled liquid V.

In contrast, no jumps appear in the curves of the Q2 process; one can observe only a small change in the slope of the curves at around 1400 K, which can be taken as the estimate of the glass transition temperature. This behavior is compatible with a second-order phase transition, although one must point out that the liquid-glass transition is not a true phase transition,

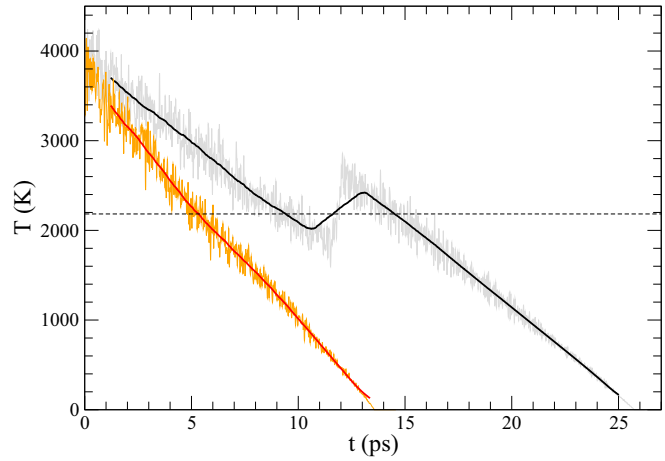

FIG. 1. Ionic temperature as a function of the MD simulation time for quenching processes Q1 (gray and black lines) and Q2 (orange and red lines), describing liquid-solid and liquid-glass transitions, respectively. The thicker black and red lines are obtained from averaging procedures to get a smoother behavior than that of the highly fluctuating rough data. The horizontal dashed line indicates the experimental melting temperature of vanadium.

but rather a rate effect [1], so that the precise value of the glass transition temperature depends on the cooling rate [19]. Our findings are in qualitative agreement with the results reported in previous *ab initio* studies on tantalum [5] and copper [6]. Due to the high computational cost (particularly for metallic systems), *ab initio* simulations are carried out by adopting relatively small supercells, so that finite-size effects are expected to be present, for instance, by lowering the free-energy barrier for the crystallization process [20]; however, since, by comparison with experimental findings, both our Q1 and Q2 simulations seem to capture the basic physical evolution processes of the system, we expect that these effects

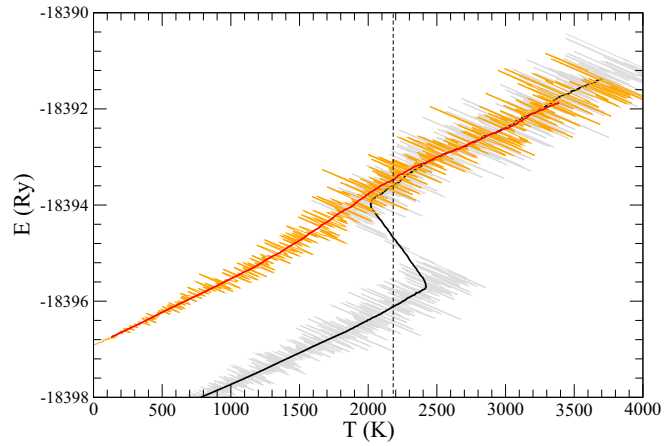

FIG. 2. System total energy as a function of the temperature for quenching processes Q1 (gray and black lines) and Q2 (orange and red lines), describing liquid-solid and liquid-glass transitions, respectively. The thicker black and red lines are obtained from averaging procedures to get a smoother behavior than that of the highly fluctuating rough data. The vertical dashed line indicates the experimental melting temperature of vanadium.

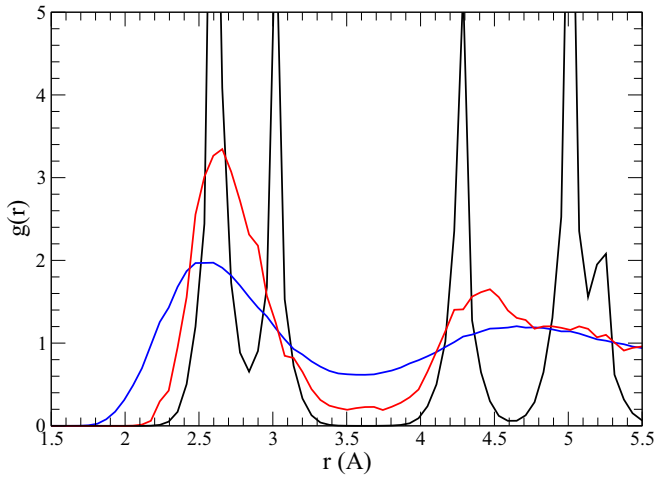

FIG. 3. Pair correlation function $g(r)$ of V in the liquid (blue line), bcc crystal (black line, Q1 quenching process), and glass (red line, Q2 quenching process) phases, obtained by averaging over 600 configurations of the MD simulations.

cannot change the basic qualitative conclusions of our work, although they can certainly hinder a precise estimate of the critical cooling rate for glass formation.

As in Ref. [5], the final densities of each simulation were obtained by relaxing the supercell volume in such a way to minimize the energy of the system. The density of the final glass configuration is estimated to be 6.07 g/cm^3, which is (about 3%) smaller than that of crystalline V, 6.25 g/cm^3 (experimental value: 6.09 g/cm^3), similar to what was observed for Ta [5].

A. Structural properties

Figure 3 reports the pair correlation function $g(r)$ of V in different phases, and the main structural parameters can be found in Table I. The liquid-phase $g(r)$ was obtained by averaging over 600 initial configurations at a temperature of about 4000 K; $g(r)$ for the bcc crystalline and glass phases were instead obtained by averaging over 600 final configurations by adopting the Q1 and Q2 quenching rates, respectively. As can be seen, the calculated $g(r)$ for liquid V is characterized by only two significant peaks, indicating a short-range order, while the peaks are clearly more numerous and sharper for the bcc crystalline phase. The position of the first peak of $g(r)$ for liquid V, found at 2.60 Å, is in perfect agreement with the value obtained by the *ab initio* simulation of Debela *et al.* [7]. Instead, in the glass phase the first peak of $g(r)$ is sharper and stronger than in the liquid phase; moreover, the second peak decomposes into two separate peaks. The splitting of the second maximum of the $g(r)$ curve into two subpeaks is recognized as a characteristic indication of amorphous solids (glasses), differentiating it from a liquid [18]. Moreover, in the glassy state the peak intensities are stronger than those in the liquid state, which implies that the glassy phase has a higher degree of order with respect to the liquid one [5,6,21]. The complex atomic configuration in metallic glasses has been interpreted globally as a combination of spherical-periodic order (SPO) and local translational symmetry (LTS) [21].

TABLE I. Structural parameters and dc electrical conductivity σ [in 10^5 $(\Omega\ \mathrm{m})^{-1}$] of V in the liquid, crystal (bcc solid), and glass phases. R_1 and R_2 (in Å) denote the positions of the first two peaks of the pair coordination function $g(r)$, while n_c is the coordination number. In parentheses the value relative to the ideal bcc structure is given.

	bcc Solid	Liquid	Glass
$g(R_1)$	9.55	1.97	3.34
$g(R_2)$	5.62	1.20	1.65
R_1	2.60	2.60	2.66
R_2	2.97	4.65	4.47
R_2/R_1	1.14 (1.15)	1.79	1.68
n_c	14.0	14.0	13.4
σ	57	12	10

In order to characterize more quantitatively the pair correlation functions of V in the different phases, it is useful to consider the quantity R_i, which represents the average distance from the ith nearest-neighbor shell to the centered atom: for instance, R_1 corresponds to the average distance of the first-nearest-neighbor shell; by normalizing all the peak positions to R_1 one can minimize the influence of the chemical composition and atomic size on the peak positions and thus extract the general features of the systems [21]. We find that $R_2/R_1 = 1.14$, 1.79, and 1.64 for the bcc solid, liquid, and glass phases, respectively; note that $R_2/R_1 = 1.15$ in an ideal bcc structure. Our liquid value is close to that (1.86) reported by Liu *et al.* [21] in metallic liquids (pure Al, Cu, and Ni metals and several multicomponent metals), and the same is true for the glass phase. In fact, as also found in Ta glass by Zhang *et al.* [5], our R_2/R_1 value is in reasonable agreement with the peak ratio rule ($R_2/R_1 \simeq \sqrt{3} \simeq 1.73$) suggested by Liu *et al.* [21]. In disordered metallic systems, such as liquids or ideal amorphous metals, spherical Friedel oscillations are formed in the effective interatomic potential which cause a SPO of atomic arrangement at the short- and medium-range distances: the SPO theory [21,22] predicts that $R_2/R_1 = 1.8$, so that the atomic distribution in the first-neighbor shells is well predicted by SPO. The slightly lower R_2/R_1 value found for the glass phase could be explained [21] by the increase of LTS imposed on the SPO where, however, the LTS represents only one-dimensional translational order along a dense-packed direction rather than three-dimensional translational periodic order in a lattice [5,21]. This is in line with the view that the glassy state is an intermediate step between the liquid and crystalline phases so that the degree of order in MGs is higher than that in liquids but still lower than that in crystals [21].

From the $g(r)$ curves the *coordination number* n_c can be estimated by integrating the area under the first peak. We find that $n_c = 14$ in the liquid phase, while it slightly decreases to $n_c = 13.4$ in the glass phase, in good agreement with the value (13.5) found by Fang *et al.* [6] for the glass phase of Cu. These values should be compared to $n_c = 14$ if one integrates the area under the first two (rather close) peaks (see Fig. 3) of the ideal bcc crystal, corresponding to the number of nearest (eight) and next-nearest (six) neighbors.

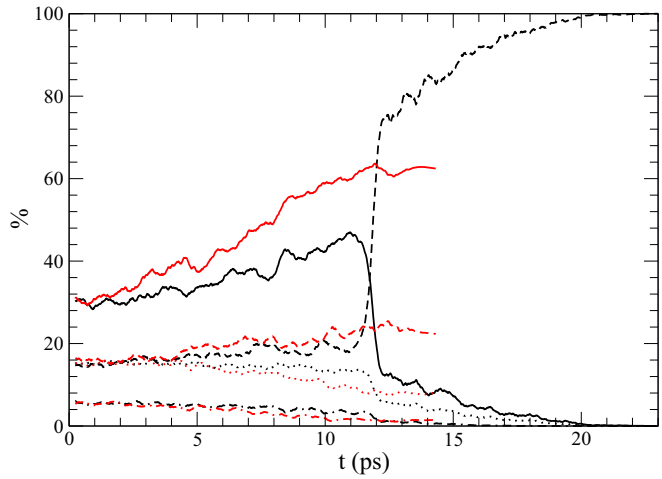

FIG. 4. Evolution, along the MD simulations, of the fraction of the main structures of V, corresponding to quenching processes Q1 (black lines) and Q2 (red lines), describing liquid-solid and liquid-glass transitions, respectively. Icosahedral structures, solid lines; bcc structures, dashed lines; tetrahedral structures, dotted lines; fcc-hcp structures, dot-dashed lines.

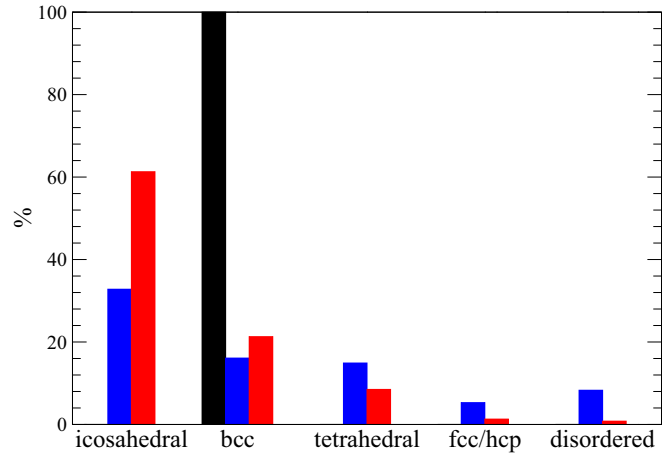

FIG. 5. Histograms indicating the fraction of the main structures of V in the liquid (blue histogram), crystal (black histogram), and glass (red histogram) phases.

The local atomic environment is investigated by the *bond-pair analysis*, which is a rather effective way for characterizing atomic clusters in condensed-matter systems [6,7,23]. One can introduce [6,23] four index numbers (i, j, l, m) to classify bonded pairs of atomic clusters: $i = 1$ if atom A and atom B form a bond; otherwise, $i = 2$. j denotes the number of near neighbors which form bonds with atoms A and B; l represents the number of bonds formed among the neighboring atoms, while m is a special classifying index parameter. Two atoms are considered to be bonded if their distance is smaller than a cutoff radius, defined by taking the first minimum of the pair correlation function. With the calculation of these index numbers, the bond pairs can be qualitatively categorized into a few distinct, fundamental structures: *icosahedral*, *tetrahedral*, *fcc-hcp*, *bcc*, and *disordered*.

In Fig. 4 we plot the evolution, along the MD simulations, of these main structural types, while Fig. 5 reports histograms indicating the fraction of such structures in the different phases. As can be seen, in the initial liquid phase the predominant structures are icosahedral in character (about 33%), although significant contributions also come from tetrahedral and bcc structures and from disordered structures too. Interestingly, as the system undergoes a phase transition to a crystalline state, by adopting the Q1 quenching rate, a sudden change occurs in the fractions of different structures: in less than 10 ps, essentially, they all become bcc in character. This behavior is very similar to that observed for the liquid-solid transition in the *ab initio* study of Debela *et al.* [7]. Interestingly, at our estimated melting temperature of about 2200 K, in good agreement with the experimental one (2183 K), one can observe that the fraction of icosahedral structures becomes equal to that of bcc type.

However, if the quenching rate is sufficiently fast, as in the Q2 process, the behavior turns out to be completely different: the fraction of icosahedral structures smoothly increases by cooling the system in such a way that it is almost twice the value of the liquid phase (about 61%) at the end of the simulation, the fraction of disordered structures dramatically decreases, and the sum of the fractions relative to tetrahedral and bcc structures remains almost constant. Therefore, the transition from the liquid to glass state can be characterized in terms of a considerable increase in icosahedral structures, in line with what was found in Ta [5]. Since an icosahedron is a rather good approximation to an isotropic sphere, icosahedral arrangements of atoms turn out to be the best configurations to optimize close packing [18].

The angle distribution function $g_3(\theta, r_m)$ is shown in Fig. 6; it measures triplet correlations: θ indicates the angle between the two vectors that join a central particle with two neighbors at a distance smaller than r_m, where the cutoff value r_m is taken as the position of the first minimum of the corresponding $g(r)$ function. As can be see, the $g_3(\theta, r_m)$ function for glass V is

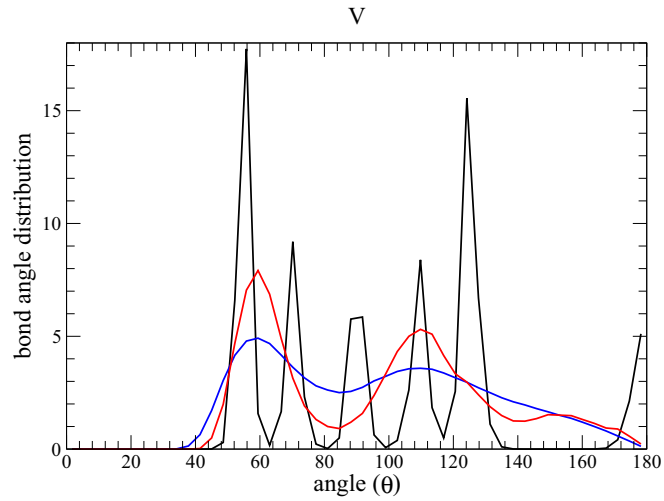

FIG. 6. Angle distribution function $g_3(\theta, r_m)$ of V in the liquid (blue line), crystal (black line), and glass (red line) phases (see text for definition). The cutoff distance r_m is taken as the position of the first minimum of the corresponding $g(r)$ function.

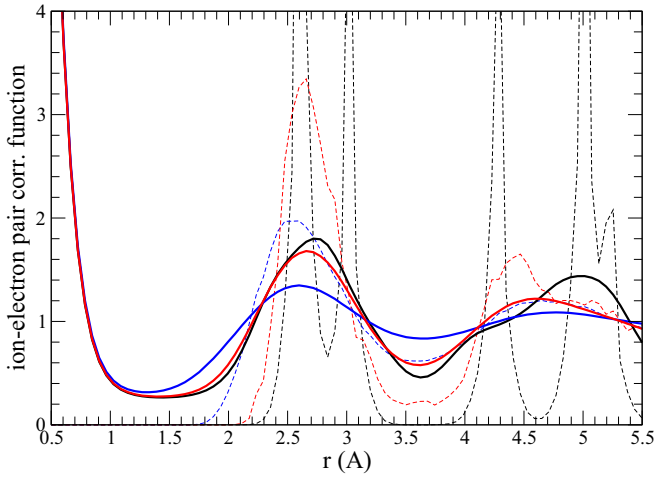

FIG. 7. Electron-ion pair correlation function $g_{ei}(r)$ relative to a single configuration of V in the liquid (blue line), crystal (black line), and glass (red line) phases (see text for definition). Dashed lines denote the corresponding $g(r)$ curves of Fig. 3.

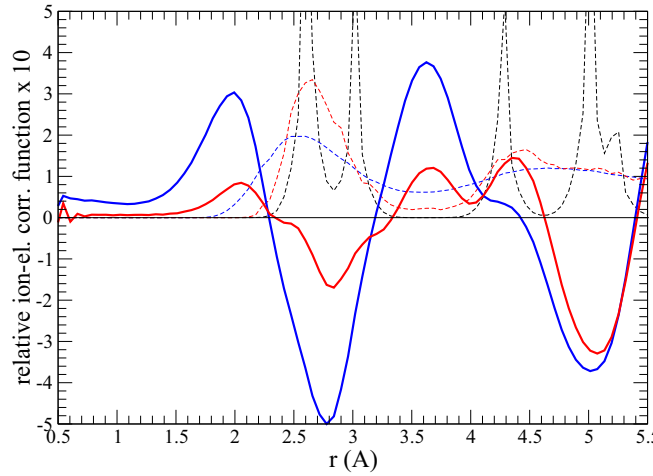

FIG. 8. Difference (magnified by a factor of 10) between $g_{ei}(r)$ and the same function evaluated in the bcc solid phase, $\delta g_{ei}(r)$, relative to a single configuration of V in the liquid (blue line) and glass (red line) phases. Dashed lines denote the corresponding $g(r)$ curves of Fig. 3.

qualitatively similar to that of the liquid phase (the two main peaks are just more pronounced) but markedly different from that of the bcc crystal. Interestingly, the first peak at about 60° is compatible with configurations in which icosahedral structures are predominant: in fact, a regular icosahedron has five equilateral triangular faces meeting at each vertex.

B. Electronic properties

In Fig. 7 we report the electron-ion pair correlation function $g_{ei}(r)$, which describes [10,11] the correlation between the local density of the electrons and the local density of the ions; we remember that 13 (8 core + 5 valence) electrons per V atom are explicitly considered in our calculations. Basically, the $g_{ei}(r)$ curves exhibit Friedel-like fluctuations, with a strong, short-distance peak due to the core electrons localized around each V ion and other peaks which somehow reflects the corresponding behavior of the $g(r)$ curves. The presence of interatomic metallic bonds can be inferred from the appreciable amount of electronic charge observed in the interstitial regions. Moreover, by considering $\delta g_{ei}(r)$, defined as the difference between $g_{ei}(r)$ and the same function evaluated in the bcc solid phase, one can emphasize (see Fig. 8) the differences among the $g_{ei}(r)$ curves; note that, particularly in the liquid phase, a significant amount of electron density accumulates in regions between the $g_{ei}(r)$ peaks, leading to a slightly more uniform electron-charge distribution than in the bcc solid phase.

As described in the previous section, using the Kubo-Greenwood approach, the dc electrical conductivity $\sigma(\omega = 0)$ can be calculated by extrapolating the optical conductivity expression for finite ω. In Fig. 9 the behavior of the frequency-dependent conductivity $\sigma(\omega)$ is reported, considering a single configuration of V in the liquid, crystal, and glass phases. This procedure is justified because, in the crystal and glass phases, the temperature of the system is so low that the atoms are essentially frozen, so that considering multiple configurations would not lead to appreciable changes in the $\sigma(\omega)$ curves.

As can be seen from Fig. 9 (see also data in Table I), our estimate for the dc electrical conductivity in V bcc crystal, 57×10^5 $(\Omega\ \mathrm{m})^{-1}$, is in good agreement with the reference experimental value [24], 50×10^5 $(\Omega\ \mathrm{m})^{-1}$. Moreover, the $\sigma(\omega)$ curves for liquid and glass V are quite similar; as a consequence, the estimates for the dc electrical conductivity are also comparable: 12×10^5 $(\Omega\ \mathrm{m})^{-1}$ for liquid V and 10×10^5 $(\Omega\ \mathrm{m})^{-1}$ for glass V. Both these values are substantially lower than that for the bcc crystal, as can be expected from the higher degree of disorder characterizing the liquid and glass phases.

Similar considerations hold for the electron thermal conductivity K_e, which can be assumed to be proportional to the electrical conductivity because the Wiedemann-Franz law can also be applied to metallic glass systems [2,25,26]. Our estimated room-temperature K_e is 37 W/mK for the bcc

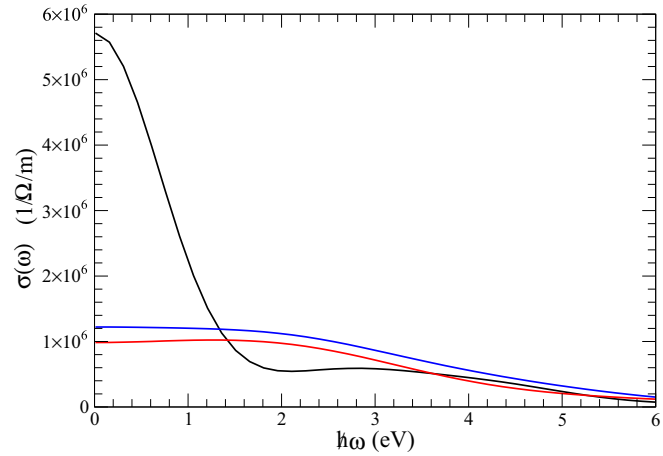

FIG. 9. Optical conductivity $\sigma(\omega)$ relative to a single configuration of V in the liquid (blue line), crystal (black line), and glass (red line) phases, (see text for definition).

crystal, in good agreement with the experimental value of 35 W/mK [27], while, instead, $K_e = 6$ W/mK for the glass phase.

IV. CONCLUSIONS

In conclusion, we have simulated, by *ab initio* molecular dynamics, the formation of a metal glass of vanadium and computed different structural, energetic, and electronic properties which were compared to those of vanadium in the standard, solid-state, bcc crystal phase (obtained by adopting a slower quenching rate) and in the liquid phase too. As found for other monoatomic metallic glasses, we have shown that the fundamental structural process of V glass formation is represented by the tendency of V atoms to form icosahedral structures. Detailed analysis of the electronic properties, such as the electronic-charge distribution and the electrical and thermal conductivities, indicates they are qualitatively similar in the glass and liquid phases and suggests that the glass state of vanadium can indeed be interpreted as a "frozen" (inherent) liquid configuration.

[1] J. Schroers, Phys. Today **66**(2), 32 (2013); Nature (London) **512**, 142 (2014).

[2] L. Zhong, J. Wang, H. Sheng, Z. Zhang, and S. X. Mao, Nature (London) **512**, 177 (2014).

[3] D. Turnbull, Contemp. Phys. **10**, 473 (1969).

[4] L. A. Greer, Science **267**, 1947 (1995).

[5] J. C. Zhang, C. Chen, Q. X. Pei, Q. Wan, W. X. Zhang, and Z. D. Sha, Mater. Des. **77**, 1 (2015).

[6] H. Z. Fang, X. Hui, G. L. Chen, and Z. K. Liu, Phys. Lett. A **372**, 5831 (2008).

[7] T. T. Debela, X. D. Wang, Q. P. Cao, D. X. Zhang, and J. Z. Jiang, J. Phys.: Condens. Matter **26**, 155101 (2014).

[8] P. Giannozzi, S. Baroni, N. Bonini, M. Calandra, R. Car, C. Cavazzoni, D. Ceresoli, G. L. Chiarotti, M. Cococcioni, I. Dabo, A. Dal Corso, S. Fabris, G. Fratesi, S. de Gironcoli, R. Gebauer, U. Gerstmann, C. Gougoussis, A. Kokalj, M. Lazzeri, L. Martin-Samos, N. Marzari, F. Mauri, R. Mazzarello, S. Paolini, A. Pasquarello, L. Paulatto, C. Sbraccia, S. Scandolo, G. Sclauzero, A. P. Seitsonen, A. Smogunov, P. Umari, and R. M. Wentzcovitch, J. Phys.: Condens. Matter **21**, 395502 (2009).

[9] H. J. Monkhorst and J. D. Pack, Phys. Rev. B **13**, 5188 (1976).

[10] P. L. Silvestrelli, A. Alavi, and M. Parrinello, Phys. Rev. B **55**, 15515 (1997).

[11] P. L. Silvestrelli, Phys. Rev. B **60**, 16382 (1999).

[12] J. P. Perdew, K. Burke, and M. Ernzerhof, Phys. Rev. Lett. **77**, 3865 (1996).

[13] P. Ganesh and M. Widom, Phys. Rev. B **77**, 014205 (2008).

[14] See Supplemental Material at http://link.aps.org/supplemental/10.1103/PhysRevB.99.094201 for dynamical, energetic, and structural properties obtained in the spin-polarized simulation of the glass-forming (Q2) process, compared to those relative to the unpolarized one.

[15] R. Kubo, J. Phys. Soc. Jpn. **12**, 570 (1957); D. A. Greenwood, Proc. Phys. Soc. **71**, 585 (1958).

[16] L. Calderin, V. V. Karasiev, and S. B. Trickey, Comput. Phys. Commun. **221**, 118 (2017).

[17] N. D. Mermin, Phys. Rev. **137**, A1441 (1965).

[18] P. J. Steinhardt, D. R. Nelson, and M. Ronchetti, Phys. Rev. B **28**, 784 (1983).

[19] K. Niss and T. Hecksher, J. Chem. Phys. **149**, 230901 (2018).

[20] H. Niu, P. M. Piaggi, M. Invernizzi, and M. Parrinello, Proc. Natl. Acad. Sci. USA **115**, 5348 (2018).

[21] X. J. Liu, Y. Xu, X. Hui, Z. P. Lu, F. Li, G. L. Chen, J. Lu, and C. T. Liu, Phys. Rev. Lett. **105**, 155501 (2010).

[22] P. Häussler, Phys. Rep. **222**, 65 (1992).

[23] J. D. Honeycutt and H. C. Andersen, J. Phys. Chem. **91**, 4950 (1987).

[24] C. Kittel, *Introduction to Solid State Physics*, 7th ed. (Wiley, New York, 1996), p. 160.

[25] C. L. Choy, W. P. Leung, and Y. K. Ng, J. Appl. Phys. **66**, 5335 (1989).

[26] T. Mizoguchi, T. Kudo, and S. Takayama, J. Phys. (Paris) Colloq. **41**, C8-501 (1980).

[27] W. D. Jung, F. A. Schmidt, and G. C. Danielson, Phys. Rev. B **15**, 659 (1977).